Estimating Q from Hydraulic Fracture Related Seismicity

Gisela Viegas*, ESG, Kingston, Ontario, Canada
Gisela.Fernandes@esgsolutions.com
and
Adam Baig, ESG, Kingston, Ontario, Canada,Ted Urbancic, ESG, Kingston, Ontario, Canada
Eric von Lunen, Nexen, Calgary, Canada, Jason Hendrick, Nexen, Calgary, Canada, Sean Lovric, Nexen Calgary

Summary

Attenuation plays a major role in earthquake seismology affecting the way the seismic energy is dissipated during wave propagation. If not properly accounted for attenuation can bias calculations of earthquake source parameters and physical properties. We accurately estimate source parameters of micro-seismic events recorded during an hydraulic fracturing completion program in a shale reservoir and determine whole-path attenuation measurements for the region. We use a simultaneous inversion method (NetMoment) which takes advantage of the large number of recording sensors and of the commonality of the earthquake source to avoid biasing the source and attenuation measurements. We improved the accuracy in the NetMoment results by imposing constraints derived from the statistical analysis of the data. Our source results indicate that the micro-seismic events have on average low stress drops (1.5 MPa), lower than the stress drop of natural tectonic micro-earthquakes occurring in similar tectonic settings (~17 MPa), and follow self-similar scaling relationships. We observe that high frequency attenuation is variable within small volumes and its variability can be further used to improve geophysical models of hydrocarbon reservoirs and identify its three dimensional shape and regions saturated/depleted of hydrocarbons or fluids.

Introduction

Seismic attenuation, a combination of energy dissipation by frictional heating and energy scattering by heterogeneities presents in the medium, affects the characteristics of the propagating seismic waves and if not properly accounted for, can bias measurements of earthquake source parameters and physical properties. Attenuation is often represented by its quality factor, *Q*, which is a dimensional variable, inversely proportional to attenuation, and measures the fractional loss of strain energy per oscillation cycle. During propagation, higher frequencies (shorter wavelength) are generally more attenuated than the lower frequencies (longer wavelength), simply because it oscillates more cycles over the same path length. This effect reduces the high frequency content of the signal and strongly impacts the shape of its source spectrum. *Q* depends on and is sensitive to rock rheology (porosity, viscosity, fracture content, fracture aspect ratios, etc.), and local pressure, temperature and fluid saturation conditions and, in general, increases with material density and velocity as a function of burial depth (confining pressure). Typical *Q* values for crustal rocks increase with increasing density, ranging from 30 (shale) to 250 (granite) for P waves, and from 10 (shale) to 150 (granite) for S waves (Lay and Wallace, 1995).

Source characteristics of seismic events such as seismic moment, fault radius, stress drop, radiated energy, etc., are commonly calculated in the frequency domain from the displacement amplitude spectrum of P and/or S waves. Seismic moment is based on the low frequency plateau observed in the source spectrum (low-frequency plateau), whereas source dimension is related to the transition from the low frequency plateau to the high frequency drop-off in the source spectrum, referred to as the corner frequency, and the calculation of radiated energy entails integrating the entire band of the source spectrum (energy flux). One long-standing problem is how to accurately correct for attenuation and thereby avoid biasing any source parameter calculations. This problem becomes critical in the study of micro-earthquakes because they generate high frequency signals (100 Hz to 1000 Hz) that are heavily attenuated. The task is not easy as a trade-off exists between attenuation and the apparent corner frequency (Anderson and Hough, 1984), and many possible combinations of these two variables provide equally good solutions that fit the source spectra equally well (Hough et al., 1991). Alternative methods to the individual fitting method have been developed to avoid the trade-off pitfall. Most of these methods use spectral ratios, empirical Green's functions or statistical approaches on large amounts of data. In this study we analyse seismic data recorded during a hydraulic fracture stimulation using a spectral method designated by NetMoment (Hutchings, 2001; Gok et al., 2009) coupled to a statistical analysis of the results.

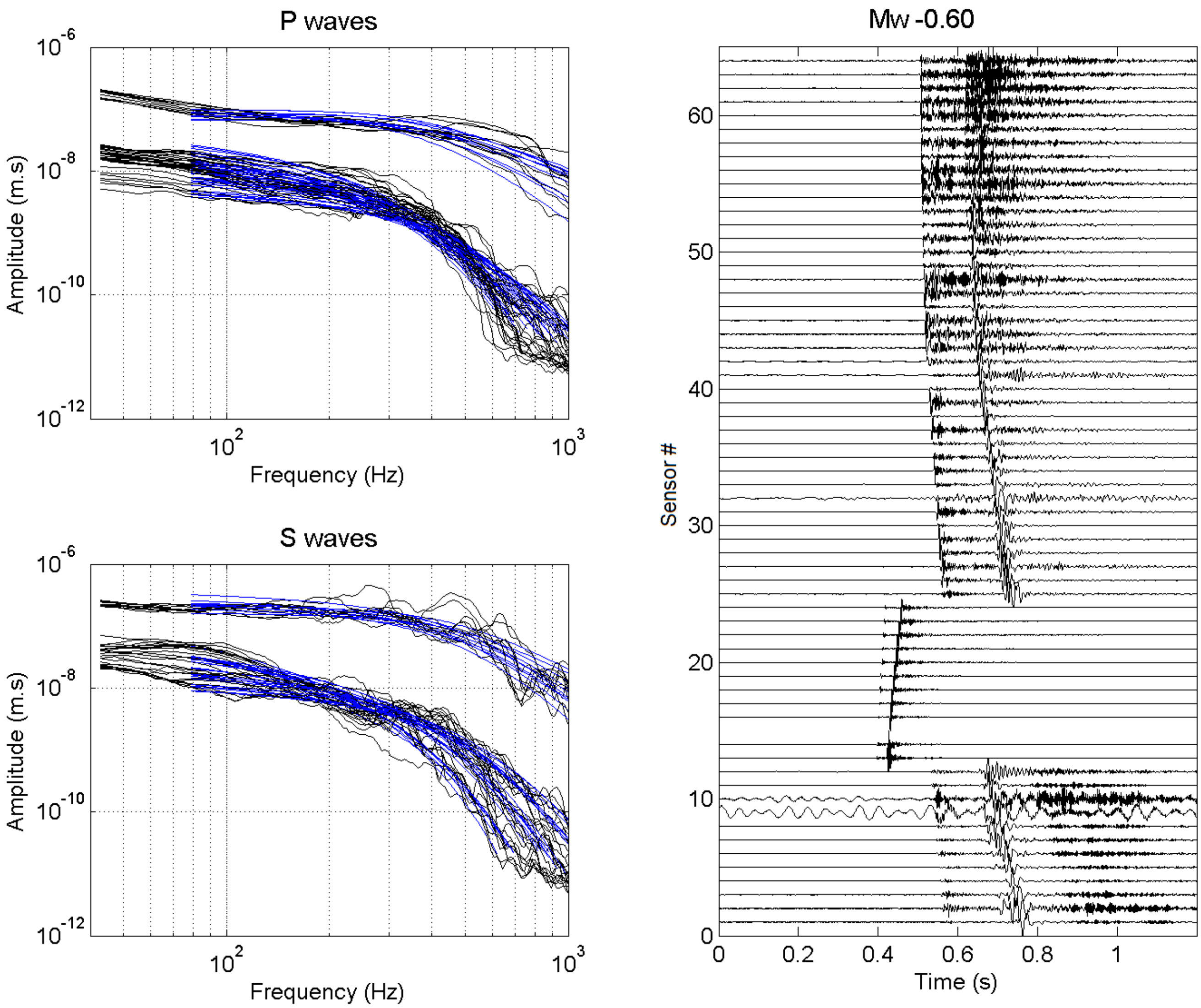

Figure 1: NetMoment method. Example of the simultaneous inversion for source, site and path attenuation of a Mw-0.6 event recorded at 63 downwhole sensors. The P- and S-spectrum from each sensor is fitted to Boatwright-spectrum (blue lines). The frequency-range for each individual fit is different depending on the signal to noise ratio for each sensor.

NetMoment Method

The NetMoment method uses spectra of direct P and S waves and simultaneously inverts for micro-earthquake source properties (seismic moment and corner frequency) and medium attenuation. The simultaneous inversion is based upon the commonality of the earthquake source, and the assumption that the source corner frequencies from a particular earthquake will have the same value at each site and the differences in spectra can be attributed to the propagation path and individual site responses. We apply the method by simultaneously fitting the instrument-corrected displacement spectra recorded at all available stations of one micro-earthquake at a time, solving for its corner frequency, the long period level (low frequency plateau) at each station and the combined site-specific and whole-path attenuation factor for each source-station path. We further fit the spectra using Boatwright's (1980) source spectrum model. Figure 1 illustrates the implementation of the NetMoment method using a Mw-0.6 micro-seismic event recorded with 3 downhole arrays. The NetMoment method performs best if wide distributions of sensors are available so that different source-station paths with different attenuation characteristics are captured. In this way the trade-off between attenuation and corner frequency is not the same for all paths and an apparent corner frequency estimate can be avoided. The processing workflow of the NetMoment method is automated and particularly useful when dealing with large datasets such as the ones from hydraulic fracture completions that can consist of several tens of thousands of micro-seismic events.

NetMoment Application to a Hydraulic Fracturing Treatment Dataset

We investigate the source parameters and source-station *Q* of a large dataset of micro-seismic events (>20,000 events) generated during a hydraulic fracturing completion program in the Horn River Basin, British Columbia, Canada, using the NetMoment method. The events were recorded with several string arrays of 15 Hz geophones deployed in deep boreholes. The data was sampled at 4000 Hz. Figure 2 shows Q_P and Q_S values obtained for a sub-dataset of 700 events, clustered in space. A clear variation of both Q_P and Q_S with hypocentral distance is observable, indicating that *Q* is sensitive to the physical properties of the local layered rock formations. *Q* is smaller for the closest array (sensors 1-9) for which most of the propagation path is vertical, and increases with increasing horizontal distance in the second array. A possible explanation for this effect is that the path traveled by the propagating waves to the closest sensors is mostly vertical, through the more surficial rock formations, where most of the attenuation occurs. The path to the more distant sensors is mostly horizontal and the waves spend more time propagating in the deeper layers, where attenuation is weaker. Also observable is that the attenuation of the P waves is higher than that of the S waves for the same hypocentral distances (Q_P is lower than Q_S), which is not usually the case and is likely related with the presence of fluids.

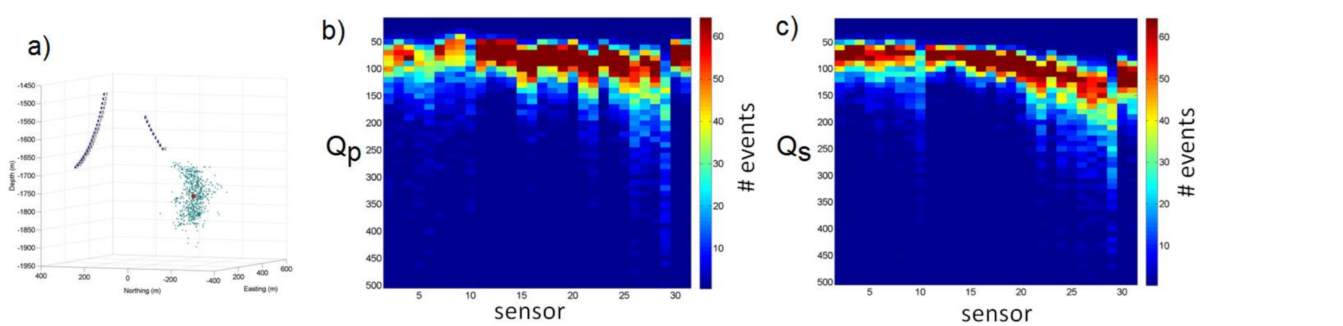

Figure 2: Q_P and Q_S values obtained for a sub-dataset of 700 events. a) 3D volume containing the recording sensors (numbered black circles) and micro-seismic events (blue circles). The red circle indicates the spatial centroid of the event cloud. Sensors in the array located on right hand side of the volume are numbered 1-9, and the ones on the left hand side of the volume 10 to 31. Numbering increases with increasing depth. b) Q_P density plot showing the distribution of events with similar whole-path Q_P (binned in intervals of 10) for each sensor. c) Q_S density plot, same as Q_P.

Although *Q* estimates are consistent for spatially clustered clouds of events they still carry uncertainties and some scatter is still observed. We therefore use statistical tools to improve the accuracy of *Q* and source parameters by imposing further constrains on the quality of the inversion. Figure 3 shows Q_P and Q_S obtained for ~4000 events for ray-paths back to one sensor. *Q* can reveal important geophysical features of the reservoir, such as for example, asperities that act as barriers in the flow pathways and prevent hydrocarbon recovery, zones of hydrocarbon saturation, etc. Attenuation together with velocity data provide further constraints on the geophysical properties of the reservoir.

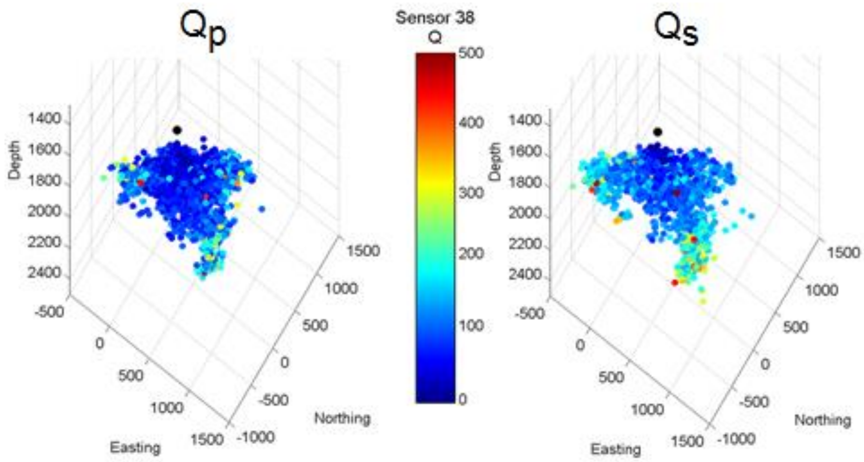

Figure 3: 3D volume containing Q_P and Q_S measurements for ~4000 events for ray-paths back to one sensor (black circle).

Source parameters are calculated using standard relationships. Seismic moment is calculated following Brune (1970), fault radius assuming Madariaga's (1976) dynamic solution for a circular fault model, and static stress drop using Eshelby's (1957) circular static crack solution. Figure 4 shows the corner frequency and stress drop measurements obtained for all the micro-earthquakes analyzed with the automated NetMoment method. We see that the self-similarity relationship holds and observe constant scaling of stress drop and micro-earthquake size, within scatter. The micro-earthquakes induced by hydraulic fracturing have on average a stress drop of 1.5 MPa, smaller than the average stress drop of natural occurring tectonic earthquakes (~17 MPa).

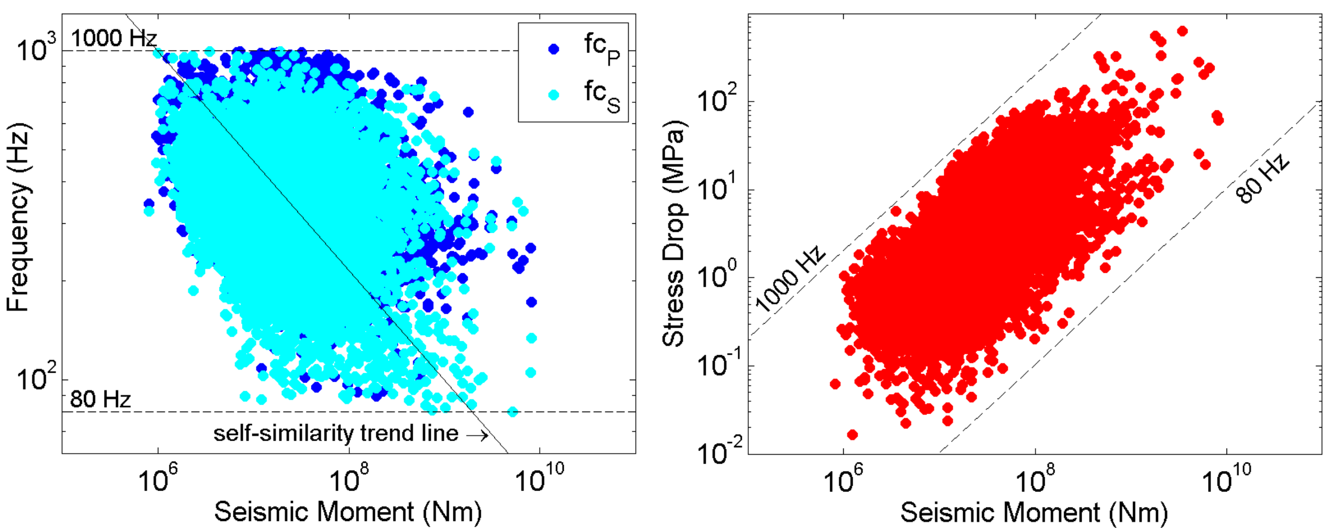

Figure 4: Corner frequency (left) and stress drop (right) measurements obtained after imposing statistical constrains in the results obtained with the NetMoment method.

Conclusions

We accurately estimate source parameters of micro-seismic events recorded during an hydraulic fracturing completion program and whole-path attenuation measurements for the region using an simultaneous inversion method (NetMoment). The method takes advantage of the large number of recording sensors and of the commonality of the earthquake source to avoid bias in the source and attenuation measurements, as introduced by a tradeoff effect between attenuation and corner frequency. Our results indicate that these induced micro-seismic events have on average lower stress drops (1.5 MPa) than natural occurring tectonic micro-earthquakes occurring in similar tectonic settings (~17 MPa), and follow self-similar scaling relationships. We observe that high frequency attenuation is variable within small volumes and its variability can be further used to improve the geophysical model of the hydrocarbon reservoir and identify its three dimensional shape and possible areas saturated/depleted with hydrocarbons or fluids.

References

Aki, K., and P. Richards, 1980, *Quantitative Seismology: theory and methods*: 932 pp., Freeman, San Francisco, California.

Anderson, J. G. and S. Hough, 1984, A model for the shape of the Fourier amplitude spectra of accelerograms at high frequencies: *Bulletin of the Seismological Society of America*, **74**, 1969-1994.

Boatwright, J., 1980, A spectral theory for circular seismic sources: simple estimates of source duration, dynamic stress drop, and radiated energy: *Bulletin of the Seismological Society of America*, **70**, 1-28.

Brune, J., 1970, Tectonic stress and the spectra of seismic shear waves from earthquakes: *Journal of Geophysical Research*, **75**(26), 4997-5009.

Eshelby, J. D., 1957, The determination of the elastic field of an ellipsoidal inclusion and related problems: *Proceedings of the Royal Society of London, A*, **241**, 376-396.

Gok, R., L. Hutchings, K. Mayeda, and D. Kalafat, 2009, Source parameters for 1999 North Anatolian fault zone aftershocks: *Pure and Applied Geophysics*, **166**, 547-566.

Hough, S. E., L. Seeber, A. Lerner-Lam, G. Armbruster, and H. Guo, 1991, Empirical Green's function analysis of Loma Prieta aftershocks: *Bulletin of the Seismological Society of America*, **81**, 1737-1753.

Hutchings, L., 2001, Program NetMoment, a Simultaneous Inversion for Moment, Source Corner Frequency, and Site Specific t*: *Lawrence Livermore National Laboratory, UCRLID 135693*.

Johnston, D. H., 1981, *Attenuation: A state-of-art summary: Seismic Wave Attenuation*, in Toksoz, M. N. and Johnston, D. H., Eds., *Geophysics* reprint series, No. 2: Society of Exploration Geophysics.

Madariaga, R., 1976, Dynamics of an expanding circular crack: *Bulletin of the Seismological Society of America*, **66**, 639-666.